beat, allowing us to study the molecular changes throughout a cardiac cycle. Thus, experiments were made under this condition. The x-ray beam is presumed to be passing through endocardium and left ventricle (12). Marking of the recorded region after an experiment, with an x-ray flux three orders of magnitude higher than that used for the x-ray diffraction measurement, confirmed that the beam actually passed through the left ventricular free wall.

The x-ray recording was repeated up to 10 times (average 5.3 recordings) with a horizontal shift of a mouse by 0.2 mm. The data were analyzed only when distinct diffraction from cardiac muscle was observed throughout a cardiac cycle. After dobutamine infusion, the mouse was moved vertically by about 0.2 mm to avoid radiation damage, and the recordings were repeated. No sign of radiation damage, such as broadening or weakening of the equatorial intensity profile, was seen.

Since the x-ray recording was not in synchrony with the cardiac cycle, it was necessary to determine correspondence between the x-ray frames and the cardiac cycle. At the heart rate of 400 - 500 per minute, there were 8 - 9 frames per each cycle, and 7 - 8 cycles were recorded in each x-ray recording which lasted for 15×70=1050msec. In the present study, only the data with 9 frames per cycle were analyzed. The frames that contained the R-wave in the electrocardiogram (Figure 1) were used as the first frame of a cycle (end-diastole). Then, frames in the same phase of the cycle were averaged. Thus, for each recording, a set of 9 images was obtained. As the R-wave could take place any time within a frame, the data had an ambiguity of one frame (15 msec) in time. This ambiguity is averaged out because, in total, data from 53 and 58 recordings were used for the baseline and dobutamine conditions, respectively.

Data analysis

Diffraction in the region of the x-ray pattern without contribution from skeletal muscles was circularly averaged. The background was fitted with a cubic spline function and the area above the background was used as the diffraction peak (Figure 4). The integrated area was used as the integrated intensity, and the center of gravity of the (1,0) reflection was converted to the (1,0) lattice spacing. The integrated intensity of the (1,1) reflection obtained this way is underestimated by $\sqrt{3}$ compared to that of the (1,0) reflection, because the intensity is averaged, not summed, along an arc. Thus, the (1,1) intensity was multiplied by $\sqrt{3}$. Since the intensity of each equatorial reflection depends on the thickness of the sample, which changes considerably across a heart, the ratio of the intensities of the (1,0) and (1,1) reflections (I(1,0)/I(1,1)) was

used as an index of the equatorial intensity change.

Then, data from different x-ray recordings were analyzed. Results from recordings on each mouse were averaged, providing a set of intensity ratios and lattice spacings for each mouse over frames. Then, data sets from 10 mice were treated statistically. The same procedure was used on the data taken after dobutamine infusion.

The half-time of contraction and relaxation was obtained by the following method. (1) The intensity ratio or lattice spacing in the first frame was taken as a diastolic level, (2) the smallest intensity ratio or the largest lattice spacing value was taken as a systolic level, (3) the average of the diastolic and systolic levels was taken as the mid-level, (4) the time when the intensity ratio or lattice spacing crossed the mid-level during the early or late phase of a heart beat was obtained by interpolation between frames and taken as the half-time of contraction or relaxation.

Using the ratio of the (1,0) and (1,1) intensities (I(1,0)/I(1,1)), the electron-density distribution in the transverse section of the hexagonal myofilament lattice was calculated by Fourier synthesis. From this, the mass associated with the thin filaments was estimated following the method of Haselgrove & Huxley (10) on the assumption that the lowest density in the electron-density map represented the background level. The 'apparent' thin-filament mass, thus calculated was interpreted as consisting of the thin filament and the myosin heads present in the vicinity of the thin filament. The mass of the thin filament was approximated by assuming that no myosin heads are present in the vicinity of the thin filament at the resting state. Then, by subtracting this from the 'apparent' thin-filament mass, the mass of heads associated with the thin filament was obtained. The same procedure was done with the intensity ratio obtained in the rigor state, and the total mass of heads can be obtained by assuming that all heads are attached to the thin filament. From these masses of heads, the proportion of heads present in the vicinity of thin filaments was calculated.

All data are expressed as mean ± standard deviation. Differences were analyzed using Student's paired *t*-test with $P < 0.05$ being regarded as statistically significant.

Results

Figure 2 shows x-ray diffraction patterns from a mouse heart in vivo at end-diastole and systole. Although diffraction spots from skeletal muscles are superposed, arcs of equatorial diffraction from cardiac muscles are clearly seen. The origin of the

reflection can be assigned without ambiguity because the skeletal muscle has a smaller filament lattice spacing and hence the reflections appeared at a larger radius. When the region where the equatorial reflections from cardiac muscle were strong, it was possible to subtract background from other tissues such as skin, lung and skeletal muscle (Figure 4). Figure 5a (blue points) shows the time course of changes in the (1,0)/(1,1) intensity ratio during a cardiac cycle at baseline. The diastolic intensity ratio was about 2.1 at end-diastole and decreased to a minimum of 0.8 in about 50 msec, which are comparable to the ratios observed in rat heart muscle (13).

Figure 5b (blue points) shows the time course of changes in the (1,0) lattice spacing at baseline. The lattice spacing at end-diastole was 37.2 nm and increased to 39.1 nm within about 90 msec after the R-wave in the electrocardiogram. If strict constant-volume behavior is assumed, this corresponds to about 10 % shortening of sarcomere. The lattice spacing continued to increase after the intensity ratio started to increase (that is, after the muscle began to relax), until the mitral valve opened and the left ventricular volume began to increase.

The experiment was repeated after dobutamine had been infused for 10 min (20 μg/kg/min). The heart rate did not change significantly (from 446 ± 26 to 449 ± 26 beats per minute, n = 10). The systemic blood pressure increased significantly from 83.9 ± 13.1 to 97.1 ± 14.9 mmHg (n=10). Figure 5a (red points) shows the change in the (1,0)/(1,1) intensity ratio under the influence of dobutamine. The second, third, and fourth data points between 20 and 60 msec after the R-wave were significantly lower than those in the control mouse, showing a faster and larger shift of mass of cross-bridges. Figure 5b (red points) is the time course of the (1,0) spacing change. The third and fourth data points are significantly larger than those in the control mouse, showing a faster shortening of muscle. The half-time of the reduction in the intensity ratio was significantly shortened by dobutamine (24.4 ± 1.4 to 20.3 ± 1.3 msec, n=10) and that of the lattice spacing was also shortened (52.8 ± 5.9 to 38.3 ± 1.8 msec, n=10). The half-relaxation time of the lattice spacing was significantly shorter after dobutamine (112.6 ± 3.0 to 106.8 ± 2.8 msec, n=10). Since the larger change in the lattice spacing suggests larger sarcomere shortening, the systolic intensity ratio might be affected by a larger filament overlap in the presence of dobutamine. However, since cardiac muscle normally works at a sarcomere length shorter than 2 μm where the thick and thin filaments are fully overlapped, this effect is not considered significant.

After an experiment, a mouse was killed by overdose of pentobarbital and left for 30

min. Then, a diffraction pattern in the rigor state was recorded. The (1,0)/(1,1) intensity ratio was 0.30 ± 0.08 (n = 8).

Discussion

The present study is the first to investigate myosin cross-bridge activity in a heart in a living body. As stated in Introduction, it is usually difficult to study murine, especially mouse, cardiac muscle in an isolated specimen under conditions that very closely match physiological. The present technique enables one to investigate mouse cardiac muscle under the most physiological condition, opening a way to study cardiac muscle functions of transgenic mice with x-ray diffraction.

The (1,0) lattice spacing observed in the present study (37.2 nm in diastole) is close to that reported in an isolated rat heart with saline perfusion (12), as well as in an isolated intact rat papillary muscle at a sarcomere length of 2.1 μm (7). If we assume that a mouse heart in vivo has the same sarcomere length-lattice spacing relation as an isolated rat papillary muscle, the working range of sarcomere length is between 1.9 and 2.1 μm. On the other hand, a much larger lattice spacing has been reported in a thoractomized rat (13). This may be due to a change in osmolarity which is caused by exposure of the circulatory system to the air. Although the open-chest model of rat has an advantage that pressure and volume of left ventricle can be measured easily during the x-ray measurement, it may be too invasive to study the true physiological state of the heart. The present closed-chest method and the open-chest method should be regarded complementary. A lattice spacing of 34 nm was reported in isolated intact rat trabeculae at a sarcomere length of 2.2 μm (16), which is smaller than the present value. Lattice spacing may be important in cardiac muscle because the distance between myofilaments may affect the contractile tension and play a role in the Frank-Starling's law. Previous studies to examine the effect of lattice spacing on tension development were made in skinned fibers which had a (1,0) spacing larger than 40 nm (17,18). It is desirable to investigate the effect at smaller lattice spacings which are more physiological.

The intensity ratios in diastole and systole found in the present study are generally similar to those in previous studies. It has been reported that more cross-bridges are formed in heart muscle preparations that are perfused by blood than in those perfused by saline (9). However, comparison of the results on saline-perfused rat heart (12), blood-perfused rat heart (13) and the present study on mouse heart under the normal

condition shows only small differences. Since the early studies required many contractions to record an x-ray diffraction pattern on a photographic film, deterioration of the sample was probably the major cause of low contractility observed in previous studies on saline-perfused specimens.

In isolated cardiac muscles, it has been found that adrenergic β-stimulation enhances the contractile force and makes both tension development and relaxation faster. This is explained by acceleration of calcium uptake (through phosphorylation of phospholamban) and reduction of the binding affinity of troponin-C to calcium (through phosphorylation of troponin-I) (2-4). These lead to faster development of tension, larger twitch tension, and faster decline of tension in cardiac muscle. In the present study, the shorter half-time of reduction in the intensity ratio shows a faster formation of cross-bridges with β-stimulation and the lower minimum intensity ratio shows that more cross-bridges are formed. Although the change in the intensity ratio during relaxation was not clearly accelerated, β-stimulation shortened the half-relaxation time of the lattice spacing. These results demonstrate that the changes of contractile properties previously observed in isolated muscle are actually taking place in a heart muscle in vivo.

In the present study, the blood pressure and the amount of myosin cross-bridge formation was increased by dobutamine infusion. On the other hand, the heart rate did not change, indicating that the effects of dobutamine stress were modest. Under this condition, the most interesting finding is that β-adrenergic stimulation does not affect the end-diastolic state. Especially, the lattice spacing at end-diastole was unchanged (Figure 5b). Since the lattice spacing is related to sarcomere length, this suggests that the left ventricular volume at end-diastole was unaffected. The elevation of blood pressure by ß-stimulation was simply due to recruitment of more cross-bridges in cardiac muscle of the free wall. The Frank-Starling mechanism, which would be relevant if the end-diastolic volume were larger and the sarcomere length longer, was not playing a major role.

By assuming that all myosin cross-bridges are in the vicinity of the thick filaments in a resting state and that all are bound to the thin filaments in the rigor state, it is possible to calculate the fraction of cross-bridges that are transferred to the vicinity of the thin filaments during contraction (see Methods). In canine cardiac muscle, the resting (quiescent) state may not be the same as the diastolic state (9). However, in rat heart muscle, no such evidence has been found. Thus, the diastolic ratio (the first frame in Figure 5a) is taken as the resting value. Then, the peak cross-bridge mass transfer

ratio under the normal condition is 56 % which increases to 74 % by dobutamine infusion. The increase is by 34 %, while the systemic blood pressure increased by 16 %. If we take the resting ratio as an average of those in the absence and presence of dobutamine (2.23), the increase is by 26%. In both cases, the increase in the mass transfer ratio is larger than that in the systemic blood pressure. Since the mass transfer ratio with the β-stimulation (75 %) is close to the maximum level observed in tetanus of frog skeletal muscle, the major fraction of cross-bridges is recruited for contraction. Thus, even at this modest level of stress that causes an increase in blood pressure but not in heart rate, most of the potential cross-bridge attachments have been made with few in reserve in the β-stimulated heart.

Weisberg and Winegrad (19) showed by electron microscopy that the heads of the α-isoform of myosin heavy chain are more extended from the backbone of the filament when C-protein was phosphorylated by protein kinase A. Since the α-isoform is dominant in adult mouse ventricle (20) and ß-stimulation causes C-protein phosphorylation (1,3,6), a change in the equatorial intensity ratio is expected. Although the present results do not support this observation, more studies at higher dobutamine stress are needed to clarify the effects of C-protein phosphorylation on the behavior of myosin heads.

Acknowledgements

The experiments were made with the approval of SPring-8 Program Review Committee (2002B0142-NL2-np, 2003A0079-NL2-np, 2003B0015-NL3-np, 2004B0319-NL3-np, 2005A0455-NL3-np). This work was supported by a 2002-2004 Research Grant for Cardiomyopathy (14162201-00) from the Ministry of Health, Welfare and Labor of Japan, and by grants from Uehara memorial Foundation and the Shimabara Science Promotion Foundation.

References

1. Jeacocke, S. A. and P. J. England. 1980. Phosphorylation of a myofibrillar protein of Mr 150 000 in perfused rat heart, and the tentative identification of this as C-protein. FEBS Letters 122:129-132.
2. Kranias, E. G. and R. J. Solaro. 1982. Phosphorylation of troponin I and phospholamban during catecholamine stimulation of rabbit heart. Nature 298:182-184.

3. Garvey, J. L., E. G. Kranias, and R. J. Solaro. 1988. Phosphorylation of C-protein, troponin I and phospholamban in isolated rabbit hearts. Biochem J 249:709-714.
4. Sulakhe, P. V. and X. T. Vo. 1995. Regulation of Phospholamban and Troponin-I Phosphorylation in the Intact Rat Cardiomyocytes by Adrenergic and Cholinergic Stimuli: Roles of Cyclic Nucleotides, Calcium, Protein Kinases and Phosphatases and Depolarization. Mol Cell Biochem 149-150:103-126.
5. Kentish, J. C., D. T. McCloskey, J. Layland, S. Palmer, J. M. Leiden, A. F. Martin, and R. J. Solaro. 2001. Phosphorylation of Troponin I by Protein Kinase A Accelerates Relaxation and Crossbridge Cycle Kinetics in Mouse Ventricular Muscle. Circ Res 88:1059-1065.
6. Hartzell, H. C. and L. Titus. 1982. Effects of cholinergic and adrenergic agonists on phosphorylation of a 165,000-dalton myofibrillar protein in intact cardiac muscle. Journal of Biological Chemistry 257:2111-2120.
7. Yagi, N., H. Okuyama, H. Toyota, J. Araki, J. Shimizu, G. Iribe, K. Nakamura, S. Mohri, K. Tsujioka, H. Suga, and F. Kajiya. 2004. Sarcomere-length Dependence of Lattice Volume and Radial Mass Transfer of Myosin Cross-bridges in Rat Papillary Muscle. Pflügers Arch 445:238-245.
8. Matsubara, I., N. Yagi, D. W. Maughan, Y. Saeki, and Y. Amemiya. 1989. X-ray diffraction study on heart muscle during contraction. In Muscle Energetics. R. J. Paul, G. Elzinga, and K. Yamada, editors. Alan T. Liss, Inc. New York. 481-486.
9. Matsubara, I. 1980. X-ray diffraction studies on the heart. Ann Rev Biophys Bioeng 9:81-105.
10. Haselgrove, J. C. and H. E. Huxley. 1973. X-ray evidence for radial cross-bridge movement and for the sliding filament model in actively contracting skeletal muscle. J Mol Biol 77:549-568.
11. Huxley, H. E., R. M. Simmons, A. R. Faruqi, M. Kress, J. Bordas, and M. H. J. Koch. 1983. Changes in the X-ray reflections from contracting muscle during rapid mechanical transients and their structural implications. J Mol Biol 169:469-506.
12. Yagi, N., J. Shimizu, S. Mohri, J. Araki, H. Nakajima, Y. Okumura, H. Toyota, T. Morimoto, Y. Morizane, M. Kurusu, T. Miura, K. Hashimoto, K. Tsujioka, H. Suga, and F. Kajiya. 2004. X-ray Diffraction from a Left Ventricular Wall of Rat Heart. Biophys J 86:2286-2294.
13. Pearson, J. T., M. Shirai, H. Ito, N. Tokunaga, H. Tsuchimochi, N. Nishiura, D. O. Schwenke, H. Ishibashi-Ueda, R. Akiyama, H. Mori, H. Kangawa, H. Suga, and N. Yagi. 2004. In Situ Measurements of Crossbridge Dynamics and Lattice Spacing in Rat Hearts by X-ray Diffraction: Sensitivity to regional ischemia. Circulation

109:2983-2986.

14. Inoue, K., T. Oka, T. Suzuki, N. Yagi, K. Takeshita, S. Goto, and T. Ishikawa. 2001. Present Status of high flux beamline (BL40XU) at SPring-8. Nucl Instrum Meth A 467-468:674-677.

15. Amemiya, Y., K. Ito, N. Yagi, Y. Asano, K. Wakabayashi, T. Ueki, and T. Endo. 1995. Large-aperture TV detector with a beryllium-windowed image intensifier for x-ray diffraction. Rev Sci Instrum 66:2290-2294.

16. Irving, T. C., J. Konhilas, D. Perry, R. F. Fischetti, and P. P. de Tombe. 2000. Myofilament lattice spacing as a function of sarcomere length in isolated rat myocardium. American Journal of Physiology 279:H2568-H2573.

17. Konhilas, J. P., T. C. Irving, and P. P. de Tombe. 2002. Myofilament calcium sensitivity in skinned rat cardiac trabeculae: role of interfilament spacing. Circ Res 90:59-65.

18. Wang, Y. P. and F. Fuchs. 1995. Osmotic compression of skinned cardiac and skeletal muscle bundles: effects on force generation, Ca2+ sensitivity and Ca2+ binding. Journal of Molecular and Cellular Cardiology 27:1235-1244.

19. Weisberg, A. and S. Winegrad. 1998. Relation Between Crossbridge Structure and Actomyosin ATPase Activity in Rat Heart. Circ Res 83:60-72.

20. Lyons, G. E., S. Schiaffino, D. Sassoon, P. Barton, and M. Buckingham. 1990. Developmental Regulation of Myosin Gene Expression in Mouse Cardiac Muscle. Journal of Cell Biology 111:2427-2436.

Figure 1 Legend Electrocardiogram (blue) and frame timing of the CCD camera (red) during time-resolved x-ray recording. There is noise in the electrocardiogram from the AC power line (60 Hz) but sharp QRS peaks and preceding small Q peaks are clearly seen. The rising edge of the frame timing pulses corresponds to the beginning of a new frame.

Figure 2 Legend X-ray diffraction patterns from a heart in vivo. (a) In end-diastole (first frame), (b) in systole (fourth frame). The intensity distribution is shown in pseudo-color. The four spots are from skeletal muscles. The rings in the rest of the pattern (arrows) are from cardiac muscle: the inner one is the (1,0), and the outer (1,1) equatorial reflection. These are averages of 6 diffraction patterns from a normal mouse.

Figure 3 Legend Positions of the x-ray beam relative to the left ventricle. The shaded areas represent a left ventricular free wall. The area between solid curves is a wall in diastole, while that between broken curves a wall in systole. At the position A, the beam is out of the heart. At B, the beam is passing through the epicardium in diastole but out of the heart in systole. At C, the beam is always in the wall but it is in the epicardium in diastole and in the endocardium in systole. At D, the beam is always passing through the wall on both sides of the heart. At E, the beam also passes through the wall on both sides but absorption by blood in the cavity hampers the x-ray measurement. In the actual experiment, a mouse (hence a heart) was moved relative to a fixed x-ray beam.

Figure 4 Legend Intensity profiles of the (1,0) and (1,1) equatorial peaks. (a) In end-diastole, (b) in systole. The data were from Figure 3, integrated within arcs of 10.5 o'clock through 2 o'clock and its opposite side. The background was drawn using a spline function.

Figure 5 Legend Effects of β-stimulation on the cross-bridge activity of mouse heart muscle. (a) The (1,0)/(1,1) intensity ratio, (b) the (1,0) lattice spacing. The abscissa is time after the R-wave in the electrocardiogram. Open squares represent data obtained before dobutamine infusion and filled circles after dobutamine infusion (20 μg/kg/ml). The error bars represent the standard error of the mean of data from 10 mice. The asterisks indicate the data points which are statistically different in paired *t*-tests between baseline and dobutamine data.

Figure 1

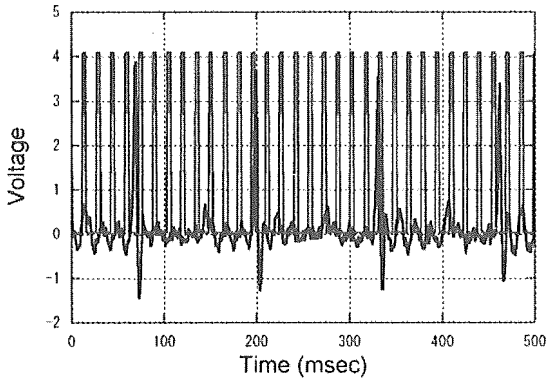

Figure 2

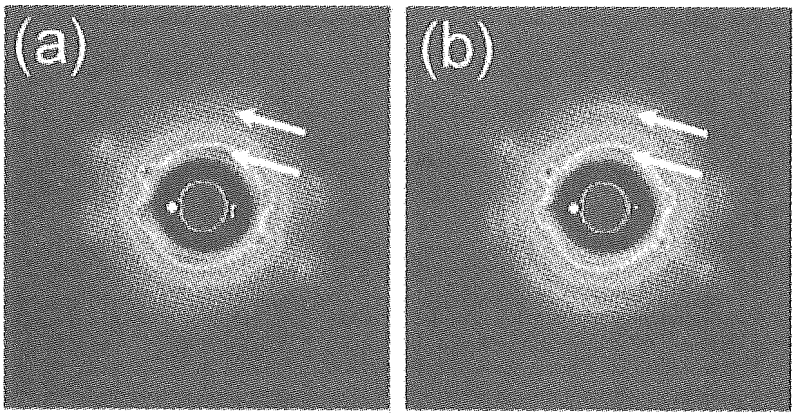

Figure 3

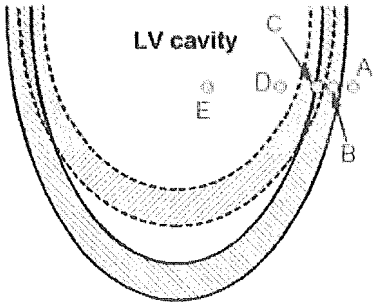

Figure 4

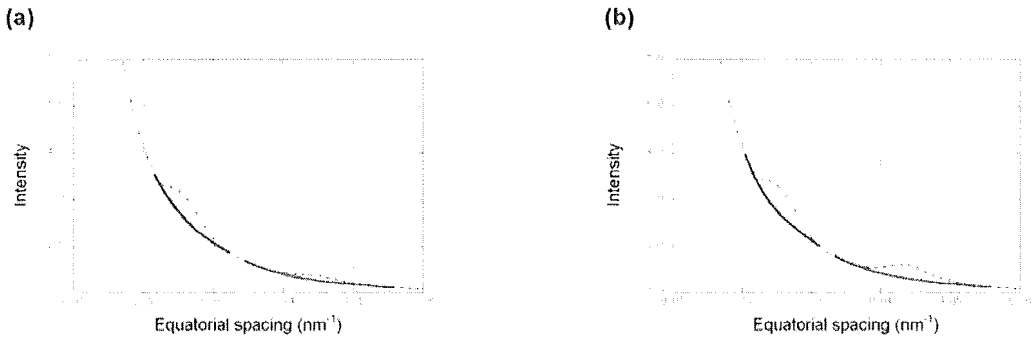

Figure 5

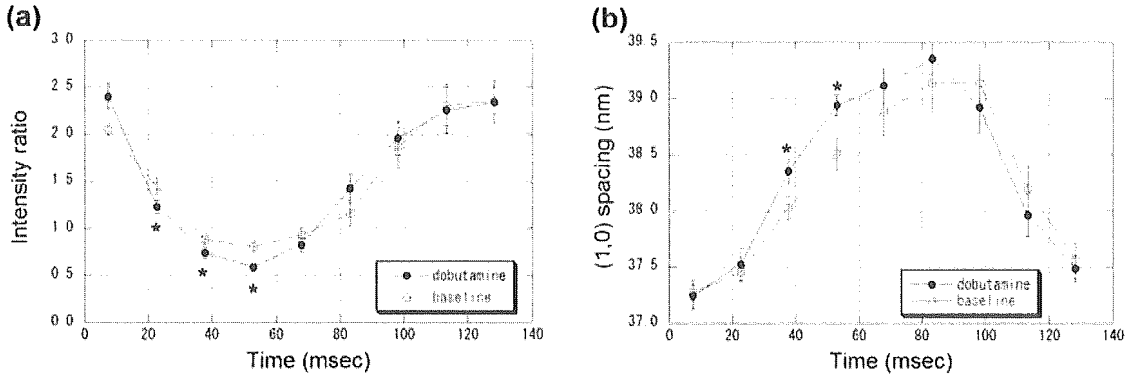

THE JOURNAL OF BIOLOGICAL CHEMISTRY
Vol. 280, No. 8, Issue of February 25, pp. 6580–6587, 2005
Printed in U.S.A.

Dantrolene Stabilizes Domain Interactions within the Ryanodine Receptor*

Received for publication, July 23, 2004, and in revised form, December 13, 2004
Published, JBC Papers in Press, December 16, 2004, DOI 10.1074/jbc.M408375200

Shigeki Kobayashi‡, Mark L. Bannister‡, Jaya P. Gangopadhyay‡, Tomoyo Hamada‡, Jerome Parness§, and Noriaki Ikemoto‡¶‖

From the ‡Boston Biomedical Research Institute, Watertown, Massachusetts 02472, the §Departments of Anesthesia, Pharmacology, Pediatrics, and Physiology and Biophysics, University of Medicine and Dentistry of New Jersey-Robert Wood Johnson Medical School, Piscataway, New Jersey 08854, and the ¶Department of Neurology, Harvard Medical School, Boston, Massachusetts 02115

Interdomain interactions between N-terminal and central domains serving as a "domain switch" are believed to be essential to the functional regulation of the skeletal muscle ryanodine receptor-1 Ca^{2+} channel. Mutational destabilization of the domain switch in malignant hyperthermia (MH), a genetic sensitivity to volatile anesthetics, causes functional instability of the channel. Dantrolene, a drug used to treat MH, binds to a region within this proposed domain switch. To explore its mechanism of action, the effect of dantrolene on MH-like channel activation by the synthetic domain peptide DP4 or anti-DP4 antibody was examined. A fluorescence probe, methylcoumarin acetate, was covalently attached to the domain switch using DP4 as a delivery vehicle. The magnitude of domain unzipping was determined from the accessibility of methylcoumarin acetate to a macromolecular fluorescence quencher. The Stern-Volmer quenching constant (K_Q) increased with the addition of DP4 or anti-DP4 antibody. This increase was reversed by dantrolene at both 37 and 22 °C and was unaffected by calmodulin. [^{3}H]Ryanodine binding to the sarcoplasmic reticulum and activation of sarcoplasmic reticulum Ca^{2+} release, both measures of channel activation, were enhanced by DP4. These activities were inhibited by dantrolene at 37 °C, yet required the presence of calmodulin at 22 °C. These results suggest that the mechanism of action of dantrolene involves stabilization of domain-domain interactions within the domain switch, preventing domain unzipping-induced channel dysfunction. We suggest that temperature and calmodulin primarily affect the coupling between the domain switch and the downstream mechanism of regulation of Ca^{2+} channel opening rather than the domain switch itself.

Dantrolene (hydrated 1-(((5-(4-nitrophenyl)-2-furanyl)methylene)amino)-2,4-imidazolidinedione sodium salt) is an intracellularly acting skeletal muscle relaxant used for the treatment of malignant hyperthermia (MH).[1] MH is a potentially deadly, pharmacogenetically mediated, hypermetabolic response to volatile anesthetics that results from unregulated intramyoplasmic Ca^{2+} release (1). The drug is known to inhibit excitation-contraction coupling of skeletal muscle (2) by suppressing depolarization-induced sarcoplasmic reticulum (SR) Ca^{2+} release in normal and MH-susceptible skeletal muscle without affecting voltage sensor activation (3). In MH, the voltage dependence of contractile activation is shifted to lower voltages (4), whereas in the presence of clinical concentrations of dantrolene, *i.e.* 10 μM (5), the voltage dependence of contractile activation is shifted to higher voltages (6, 7). Normalization of the voltage dependence of contractile activation may therefore be one of the important components of the therapeutic action of dantrolene. Dantrolene also confers a normal Mg^{2+} sensitivity to MH-susceptible muscle fibers, which would otherwise show a considerably reduced sensitivity to the normal inhibitory action of myoplasmic Mg^{2+} on the SR Ca^{2+} release mechanism (8, 9). Conferring normal Mg^{2+} sensitivity to mutated ryanodine receptor (RyR1) may be another key component of dantrolene therapeusis in MH.

Extensive studies have been carried out to examine the effect of dantrolene on the function of isolated skeletal muscle SR. It has been shown that both dantrolene and its equipotent, water-soluble analog azumolene suppress SR Ca^{2+} release induced by Ca^{2+} and various pharmacological agents (3, 10–12). Although dantrolene has been shown to suppress the ryanodine binding activity of the SR (13, 14), this finding is not universal (15). Dantrolene (1–5 μM) has been reported to have a biphasic effect on the open probability of RyR1 channels in lipid bilayers, first activating and then blocking at nanomolar concentrations (16), but others have not been able to see any effect of this drug on single channels (3). Importantly, dantrolene has been shown to at least partially restore the normal properties of RyR1 Ca^{2+} channels in SR isolated from MH-susceptible pigs (1, 17, 18). Thus, these studies together suggest that dantrolene interacts with the RyR to suppress the channel dysfunction that occurs with MH mutations.

As widely recognized, MH mutations are not randomly distributed along the RyR1 sequence. The vast majority of them are localized to two restricted regions, the N-terminal (Cys^{35}–Arg^{614}) and the central (Asp^{2129}–Arg^{2458}) domains, whereas a third, C-terminal region (Ile^{3916}–Gly^{4942}) contains fewer MH

* This work was supported by NIAMS Grants AR16922 (to N. I.) and AR045593 (to J. P.) and NHLBI Grant HL072841 (to N. I.) from the National Institutes of Health and by the Banyu Fellowship Award in Cardiovascular Medicine (to S. K.). The costs of publication of this article were defrayed in part by the payment of page charges. This article must therefore be hereby marked "*advertisement*" in accordance with 18 U.S.C. Section 1734 solely to indicate this fact.

‖ To whom correspondence should be addressed: Boston Biomedical Research Inst., 64 Grove St., Watertown, MA 02472. Tel.: 617-658-7774; Fax: 617-972-1761; E-mail: ikemoto@bbri.org.

[1] The abbreviations used are: MH, malignant hyperthermia; SR, sarcoplasmic reticulum; RyR, ryanodine receptor; MCA, methylcoumarin acetate; CaM, calmodulin; SAED, sulfosuccinimidyl 2-(7-azido-4-methylcoumarin-3-acetamido)ethyl-1,3′-dithiopropionate; CAPS, 3-(cyclohexylamino)propanesulfonic acid; AMP-PCP, adenosine 5′-(β,γ-methylene)triphosphate; MOPS, 3-(*N*-morpholino)propanesulfonic acid; BAPTA, 1,2-bis(2-aminophenoxy)ethane-*N*,*N*,*N*′,*N*′-tetraacetic acid.

mutations (19–24). The pathophysiological consequences of MH mutations are hyperactivation and/or hypersensitization of RyR1 Ca^{2+} channel activity to stimulating conditions (both pharmacological and voltage-dependent) (1, 18). In contrast, most mutations conferring susceptibility to central core disease, a rare myopathy showing a different phenotype (19, 25, 26), are located in the C-terminal putative channel pore region (Ile^{3916}–Ala^{4942}) (19, 26). The Ca^{2+} release properties of expressed RyR1 channels containing randomly selected MH mutations from the N-terminal and central domains have been shown to display similar properties of hyperactivation and hypersensitization (27). To explain these results, we have proposed a model of channel regulation that involves interdomain interactions between the N-terminal and central domains of RyR1 serving as a "domain switch" for Ca^{2+} channel regulation (28–31). In the resting state, the N-terminal and central domains make close contact at several as yet undetermined subdomains. The conformational constraints imparted by the "zipped" configuration of these two domains stabilize and maintain the closed state of the Ca^{2+} channel. Stimulation of the RyR via excitation-contraction coupling weakens these critical interdomain contacts (unzipping of the domain switch), thereby lowering the energy barrier for Ca^{2+} channel opening. Partial unzipping or weakening of the domain switch may also occur secondary to MH mutations in either the N-terminal or central domain. As a result of this, MH-susceptible RyR1 channels are hypersensitive to agonist stimuli.

Recently, Parness and co-workers (32) localized a dantrolene-binding site within the primary structure of RyR1 using [^{3}H]azidodantrolene, a pharmacologically active photoaffinity analog of dantrolene. [^{3}H]Azidodantrolene specifically photolabels the N-terminal 1400-amino acid fragment of RyR1 cleaved by an endogenous, SR membrane-bound calpain (33) and is localized within sequence Leu^{590}–Cys^{609} based on the following evidence. 1) Of several synthetic RyR1 domain peptides examined, [^{3}H]azidodantrolene specifically photolabels only peptides containing the Leu^{590}–Cys^{609} sequence (named DP1 for domain peptide-1), and 2) an anti-RyR1 monoclonal antibody recognizing DP1 inhibits [^{3}H]azidodantrolene photolabeling of RyR1 (34). The dantrolene-binding site is therefore located within the domain comprising the N-terminal portion of our proposed domain switch. Since dantrolene seems to inhibit Ca^{2+} release, these findings have led us to suggest that dantrolene may act by reinforcing interactions between the N-terminal and central portions of the RyR1 domain switch that favor a zipped conformation. Here, we present new evidence suggesting that this is indeed at least a portion of the mechanism of action of dantrolene.

In this study, we produced MH-like conditions of RyR1 (*i.e.* hyperactivation and hypersensitization of Ca^{2+} channels) in SR isolated from normal skeletal muscle by adding DP4, a synthetic domain peptide corresponding to amino acids 2442–2477 of RyR1, or anti-DP4 antibody, which, as we have recently shown, induces spectroscopic changes consistent with domain unzipping (29, 31). The magnitude of domain unzipping was determined from the accessibility of a fluorescence probe, methylcoumarin acetate (MCA), attached to the N-terminal domain, to a macromolecular fluorescence quencher (bovine serum albumin-conjugated QSY). The Stern-Volmer quenching constant (K_Q), a measure of domain unzipping, increased with the addition of either DP4 or anti-DP4 antibody. Here, we show that the addition of dantrolene reversed the increase in K_Q that was produced by DP4 or anti-DP4 antibody with an IC_{50} of 0.3 μM. This blocking effect of domain unzipping by dantrolene was present at both 37 and 22 °C and was independent of calmodulin (CaM). Although, at 37 °C, dantrolene alone inhibited DP4 enhancement of [^{3}H]ryanodine binding and activation of SR Ca^{2+} release, both measures of Ca^{2+} channel activation, it required calmodulin to do so at 22 °C. These results suggest that inhibition of RyR1 domain unzipping plays a role in the therapeutic action of dantrolene. The present data also suggest that the temperature and CaM dependence of dantrolene activity on RyR1 is due to their effects on the mechanism by which the domain switch is coupled to Ca^{2+} channel function.

EXPERIMENTAL PROCEDURES

Preparation of SR Vesicles—The SR microsomes were prepared from rabbit back paraspinous and hind leg skeletal muscles (Pel-Freez Biologicals, Rogers, AR) using the method of differential centrifugation described previously (35).

Domain Peptide and Site-specific Antibody—We used a domain peptide (DP4) corresponding to Leu^{2442}–Cys^{2477} of RyR1 both as a channel-activating reagent and as a site-directed carrier to incorporate the fluorescence probe MCA into RyR1. The peptide was synthesized on an Applied Biosystems Model 431A synthesizer, purified by reversed-phase high-pressure liquid chromatography, and evaluated by mass spectroscopy. To localize the DP4-binding site within the primary structure of RyR1, the site-specific anti-DP1 (Leu^{590}–Cys^{609}), anti-DP4 (Leu^{2442}–Cys^{2477}), and anti-DP3 (Asp^{324}–Val^{351}) polyclonal antibodies were used (31).

Site-specific MCA Labeling at the DP4-binding Site of RyR1—Site-specific fluorescence labeling of the DP4-binding sites on RyR1 in skeletal muscle SR was performed using the cleavable heterobifunctional cross-linking reagent sulfosuccinimidyl 2-(7-azido-4-methylcoumarin-3-acetamido)ethyl-1,3′-dithiopropionate (SAED) (36).

Localization of the Site of MCA Attachment within the RyR—MCA-labeled RyR1 was purified from fluorescently labeled SR using heparin and hydroxylapatite affinity columns as described by Inui and Fleischer (37). MCA-labeled RyR1 was digested with trypsin (1:100, 1:10 trypsin/protein ratio) at 22 °C for 45 min, and the resultant tryptic fragments were analyzed for fluorescence after SDS-PAGE on 8% polyacrylamide gels. For Western blot analysis, tryptic fragments were transferred to Immobilon-P membranes (Millipore Corp., Bedford, MA) at 90 V in 10% methanol and 10 mM CAPS (pH 11.0) at 4 °C. The blots were developed with anti-DP1, anti-DP3, and anti-DP4 primary antibodies and peroxidase-conjugated secondary antibodies.

[^{3}H]Ryanodine Binding Assay—Isolated skeletal muscle SR (0.5 mg/ml) that had been labeled with MCA was incubated with 10 nM [^{3}H]ryanodine (68.4 Ci/ml; PerkinElmer Life Sciences) and the desired concentration of DP4 at 22 °C for 12 h or at 37 °C for 1.5 h. Solutions contained 0.15 M KCl, 1 mM AMP-PCP, and either 10 μM dantrolene or an equivalent volume of methanol vehicle (final concentration of 0.7%) and 20 mM MOPS (pH 7.2). The [Ca^{2+}] was kept at 0.1 μM using BAPTA/calcium buffer (0.449 mM $CaCl_2$, 1 mM BAPTA, and 20 mM MOPS (pH 7.2)). The effect of CaM (1 μM) on radioligand binding was determined under identical assay conditions. Assays were carried out in duplicate according to established protocols (38), and each datum point was obtained by averaging the duplicates.

Ca^{2+} Release Assay—Isolated skeletal muscle SR (0.2 mg/ml) was incubated at 22 or 37 °C in a solution containing 0.15 M KCl, 0.1 μM Ca^{2+} (BAPTA/calcium buffer), and either 10 μM dantrolene or an equivalent volume of methanol vehicle (final concentration of 0.7%), 2.0 μM fluo-3, and 20 mM MOPS (pH 7.2) in the presence or absence of CaM. Ca^{2+} uptake was initiated by the addition of 1 mM MgATP to the cuvette, and the time course of Ca^{2+} uptake was monitored in a Cary Eclipse spectrophotometer (Varian Inc.) using fluo-3 (excitation at 488 nm and emission at 525 nm) as a Ca^{2+} indicator (31). After Ca^{2+} uptake had reached a plateau, various concentrations of DP4 were added, and the resultant Ca^{2+} release was monitored. During the Ca^{2+} uptake/release reaction, the sample was continuously stirred, and the temperature was kept constant at either 22 or 37 °C.

Spectroscopic Monitoring of Domain Unzipping—To make a macromolecular collisional quencher, QSY™ 7 carboxylic acid (2.5 mM) was conjugated with 0.5 mM bovine serum albumin by incubation in 20 mM HEPES (pH 7.5) at 22 °C for 60 min in the dark. Unreacted QSY™ 7 carboxylic acid was removed by Sephadex G-50 gel filtration. Fluorescence quenching by the conjugate was performed by measuring the steady-state fluorescence of SR labeled with MCA (excitation at 348 nm and emission at 445 nm; Cary Eclipse spectrophotometer). Fluorescently labeled SR (0.2 mg/ml) was incubated at either 22 or 37 °C in a solution containing 0.15 M KCl, 1 mM AMP-PCP, 0.1 μM Ca^{2+} (BAPTA/calcium buffer), and either various concentrations of dantrolene or an

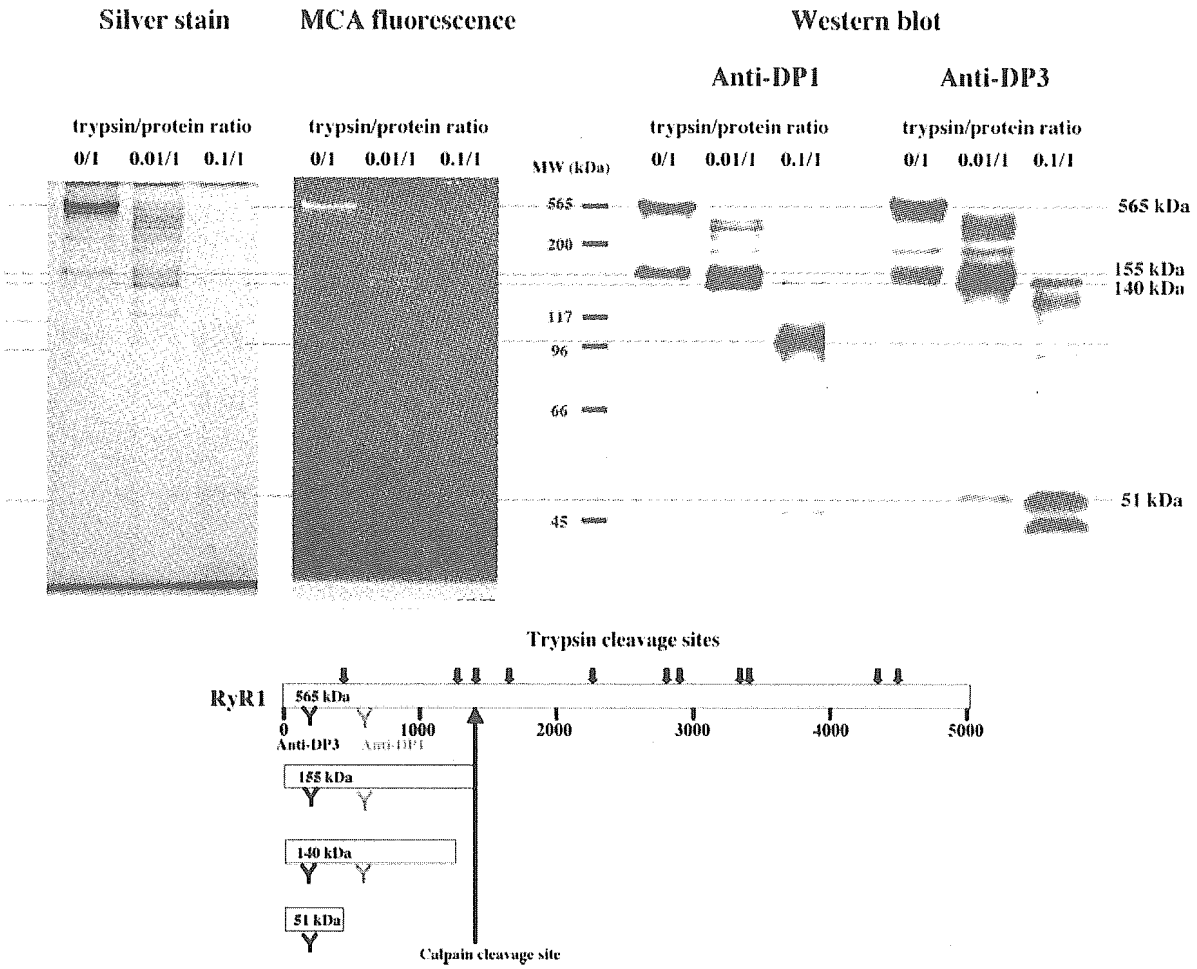

FIG. 1. **Site-directed MCA labeling of RyR1 by DP4 results in the labeling of a 51-kDa N-terminal tryptic fragment.** Purified MCA-labeled RyR1 from SR was digested with varying protein/trypsin ratios. Potential trypsin cleavage sites are denoted by the *short arrows* in the *scheme*. The epitopes for anti-DP1 and anti-DP3 antibodies are labeled with a *Y*. Note that the 51-kDa MCA-labeled fragment stained with anti-DP3 antibody, but not with anti-DP1 antibody.

equivalent volume of methanol vehicle (final concentration of 0.7%) and 20 mM MOPS (pH 7.2). Various concentrations of DP4 or 20 μg/ml anti-DP4 antibody was used to induce domain unzipping, and DP4-mut, in which one mutation was made to mimic R2458C MH mutation, was used as a negative control. The effect of dantrolene on domain unzipping was investigated by determining the effect of this drug on RyR1 MCA fluorescence in the presence or absence of 1 μM CaM. The data were analyzed using the Stern-Volmer equation: $F_0/F = 1 + K[Q]$, where F and F_0 are fluorescence intensities in the presence and absence of added quencher, respectively; K is the quenching constant, a measure of the accessibility of the protein-bound probe to the quencher; and [Q] is the concentration of the quencher (QSY) (29, 31).

RESULTS

Dantrolene Inhibits an Abnormal Unzipping of the Domain Switch—To investigate the effect of dantrolene on the mode of interdomain interaction, we utilized the MCA fluorescence quenching technique we developed to determine the extent of unzipping of the RyR1 domain switch (see "Experimental Procedures") (29, 31). As shown previously (29), DP4 mediates the specific MCA labeling of the N-terminal 1400-amino acid segment of RyR1. The precise location of DP4-mediated MCA labeling of RyR1 within the N-terminal 1400-amino acid region has not been determined, and we do not yet know whether it occurs in the N-terminal MH domain (Cys^{35}–Arg^{614}). To better define where MCA is incorporated, we used DP4 conjugated with the heterobifunctional cross-linker SAED, as a site-directing carrier, as described previously (29). The SAED-DP4 conjugate was photo-cross-linked to its binding site, and the DP4 moiety was removed under reducing conditions. MCA-labeled RyR1 was purified and subjected to tryptic digestion. The process of degradation of the fluorescently labeled polypeptide chain was then followed by SDS-PAGE. As shown in Fig. 1, partial digestion of fluorescently labeled RyR1 with a low concentration of trypsin (100:1 (w/w) RyR protein/trypsin ratio) resulted in the appearance of two major fluorescently labeled fragments with approximate molecular masses of 155 and 140 kDa. Digestion with a higher concentration of trypsin (10:1 RyR protein/trypsin ratio) resulted in the appearance of several fluorescently labeled fragments. As shown in the Western blot of Fig. 1, the 155- and 140-kDa MCA-labeled bands stained with both anti-DP1 (Leu^{590}–Cys^{609}) and anti-DP3 (Asp^{324}–Val^{351}) antibodies, whereas the 51-kDa MCA-labeled band stained with anti-DP3 antibody, but not with anti-DP1 antibody. Given the established trypsin cleavage sites of RyR1 (Fig. 1, *scheme, arrows*) (39, 40), these results suggest that the MCA-labeled RyR1 polypeptide chain degrades in the following order: 550 kDa > N-terminal 155 kDa > N-terminal 140 kDa > N-terminal 51 kDa, as illustrated in the scheme shown in Fig. 1. Since the 51-kDa MCA-labeled region is included in the N-terminal MH domain encompassed by Cys^{35}–Arg^{614}, these results indicate that DP4-mediated MCA labeling has taken place within the presumed N-terminal domain portion of the domain switch. These results also suggest that DP4, hence Leu^{2442}–Pro^{2477} of the central domain of RyR1, binds to the N-terminal domain, as predicted from our domain switch hypothesis.

The domain switch hypothesis predicts that, if the MCA probe attached to the N-terminal domain is buried in the zipped configuration, it will be relatively inaccessible to a macromolecular fluorescence quencher, bovine serum albumin-conjugated QSY. Unzipping should, however, render the MCA probe more accessible to the quencher. DP4 has been previously shown to enhance [^{3}H]ryanodine binding (28), to induce Ca^{2+} release from the SR (29), to induce contraction in skinned muscle fiber at an inhibitory Mg^{2+} concentration (41), to increase the frequency of Ca^{2+} sparks in saponin-permeabilized fibers (42), and to increase the open probability of single channels (42). Thus, DP4 mimics MH-like hyperactivation and hypersensitization of the RyR1 Ca^{2+} channel in the otherwise wild-type system. Furthermore, a mutation in DP4 (DP4-mut) that mimics the R2458C MH mutation results in virtually complete loss of the activities of wild-type DP4 (28, 29, 41, 42). This is consistent with the idea that MH mutations weaken domain-domain interactions within RyR1 that are mimicked by synthetic domain peptide-domain (RyR) interaction. Thus, we used DP4 herein to mimic MH-like channel dysfunction and to investigate the effects of dantrolene on these functions.

We first determined the fluorescence intensity of bound MCA as a function of increasing concentrations of the quencher in the absence or presence of DP4 at 22 °C. Fig. 2*A* shows the Stern-Volmer plot of fluorescence quenching of MCA attached to the N-terminal domain in the presence of various concentrations of DP4. The slope of the plot, which is equal to the Stern-Volmer quenching constant (K_Q), is a measure of the degree of domain unzipping. As shown in Fig. 2*B*, the K_Q'/K_Q value (where K_Q' is the quenching constant in the presence of DP4 or DP4-mut, and K_Q is the quenching constant in their absence) was used to assess the extent of domain unzipping. K_Q'/K_Q increased with increasing concentrations of DP4 and leveled off at ~100 μM peptide. Significantly, the DP4 concentration dependence of the increase in K_Q'/K_Q correlates well with the DP4 concentration dependence of activation of RyR Ca^{2+} channels (*cf.* Fig. 5). As shown in Fig. 2*B*, the single MH mutation in DP4-mut has made the peptide incapable of enhancing fluorescence quenching, presumably due to mutation-induced loss of affinity for the N-terminal domain. DP4-induced domain unzipping provides a simple and versatile model for the study of pathogenic and therapeutic mechanisms of MH.

We extended the above observations to investigate the effect of various concentrations of dantrolene on DP4-induced domain unzipping, again using the fluorescence quenching technique (Fig. 3). As shown in Fig. 3*A*, 1 μM dantrolene reduced K_Q from the level induced by 100 μM DP4 to near control levels. Fig. 3*B* shows the concentration dependence of the dantrolene-induced decrease in the degree of fluorescence quenching (K_Q'/K_Q). The major effect of dantrolene was seen in the concentration range of 0.1–1.0 μM, with half-maximal inhibition at 0.3 μM, agreeing well with the reported K_d of ~0.275 μM for [^{3}H]dantrolene binding to the SR (43). The maximal inhibitory effect (~73% of the control) was attained well below 10 μM, the serum concentration generally achieved during clinical treatment. Fig. 3*C* shows the effect of increasing concentrations of DP4 on K_Q'/K_Q in the presence of 10 μM dantrolene. The drug suppressed fluorescence quenching at all concentrations of DP4 tested. These results are consistent with the view that dantrolene reverses DP4-induced domain unzipping and restabilizes the zipped configuration of the domain switch.

To confirm that the observed dantrolene inhibition represents an effect on the functionality of the domain switch rather than a localized specific binding effect (*e.g.* competition with DP4 for its mating domain), we used anti-DP4 polyclonal antibody as another agent to induce domain unzipping. Like DP4,

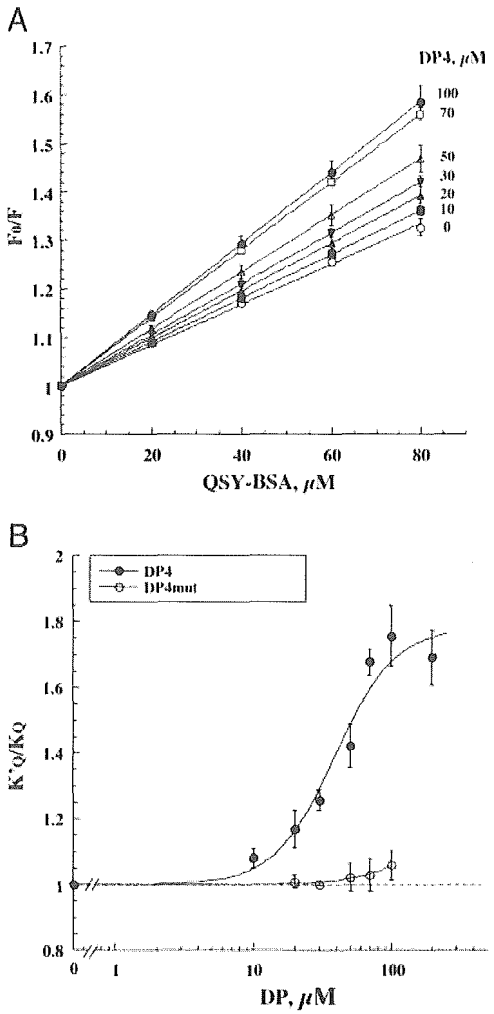

FIG. 2. **Fluorescence quenching analysis of domain unzipping by a fluorescence MCA probe attached to the RyR1 N-terminal domain.** *A*, a family of Stern-Volmer plots of fluorescence quenching as a function of increasing concentrations of a macromolecular fluorescence quencher, bovine serum albumin (*BSA*)-conjugated QSY, in the presence of increasing concentrations of DP4. The slope of each plot, which is equivalent to the Stern-Volmer quenching constant (K_Q), was used to assess the degree of fluorescence quenching. *B*, K_Q'/K_Q *versus* synthetic domain peptide concentrations. K_Q' and K_Q are the Stern-Volmer quenching constants in the presence and absence of various concentrations of DP4 (●) or DP4-mut (○), respectively. DP4 increased the extent of domain unzipping in a concentration-dependent manner, leveling off at ~100 μM. DP4-mut had no effect. Each datum point represents the mean ± S.D. obtained from at least four different experiments.

anti-DP4 antibody induces domain unzipping and also produces MH-like hyperactivation and hypersensitization effects (31) by binding to the central domain portion of the domain switch. Anti-DP4 antibody (20 μg/ml) was added to MCA-labeled SR in the absence or presence of increasing concentrations of dantrolene, and the magnitude of macromolecular fluorescence quenching was determined (Fig. 4). Here, too, dantrolene inhibited anti-DP4 antibody-induced enhancement of macromolecular fluorescence quenching. The concentration dependence of dantrolene inhibition of anti-DP4 antibody-induced fluorescence quenching parallels that of its inhibition of DP4-induced activity, *i.e.* it occurred in the concentration range of 0.1–1.0 μM, with half-maximal inhibition at 0.3 μM. In this case, however, the extent of inhibition was significantly greater than when "domain unzipping" was produced by DP4. In all the experiments above, the addition of 10 μM dantrolene in the absence of DP4 (Fig. 3*B*) or anti-DP4 antibody (Fig. 4) produced no significant effect on K_Q'/K_Q.

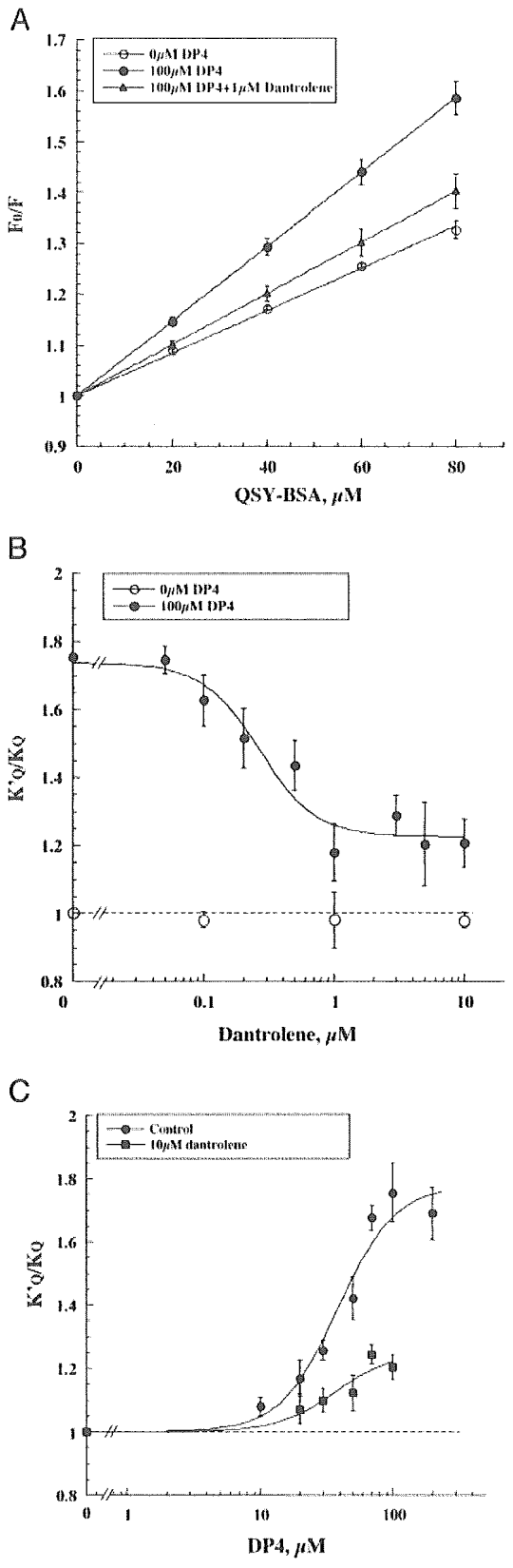

FIG. 3. **Dantrolene inhibits macromolecular fluorescence quenching induced by DP4.** *A*, Stern-Volmer plots of fluorescence quenching in the absence and presence of dantrolene. Dantrolene (1 μM) reduced the DP4-maximized K_Q' toward control values. *BSA*, bovine serum albumin. *B*, the concentration dependence of the dantrolene-induced decrease in the degree of domain unzipping (K_Q'/K_Q) (●). The effect of dantrolene was seen between 0.1 and 1.0 μM. Half-maximal inhibition occurred at 0.3 μM, and the maximal effect occurred at ~1 μM. Dantrolene produced no effect on K_Q'/K_Q in the absence of DP4 (○). *C*, effect of increasing concentrations of DP4 on K_Q'/K_Q in the presence of 10 μM dantrolene. The drug suppressed fluorescence quenching at all concentrations of DP4. Each datum point represents the mean ± S.D. obtained from at least four different experiments.

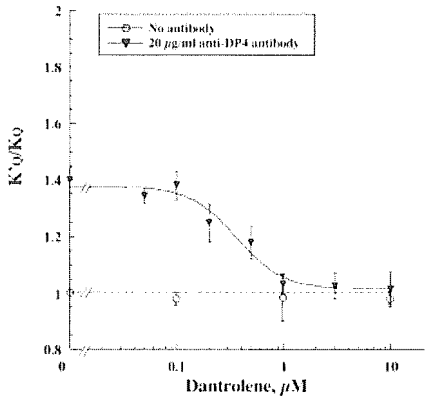

FIG. 4. **Dantrolene inhibits macromolecular fluorescence quenching induced by anti-DP4 antibody.** Shown is the concentration dependence of the dantrolene-induced decrease in the degree of domain unzipping (K_Q'/K_Q) (▼). Dantrolene produced no effect on K_Q'/K_Q in the absence of antibody (○). Each datum point represents the mean ± S.D. of at least four experiments.

According to the literature, higher temperature (37 °C) (*cf.* Refs. 7, 12, 13, and 45) and calmodulin (14) are required for significant inhibition of RyR1 Ca^{2+} channels by dantrolene. We investigated the effect of 10 μM dantrolene on domain unzipping (K_Q'/K_Q) induced by 100 μM DP4 at both 22 and 37 °C. As shown in Table I, raising the temperature from 22 to 37 °C produced only a statistically insignificant increase in the extent of dantrolene inhibition of domain unzipping from 73.7 ± 10.9 to 80.9 ± 7.4%. The addition of 1 μM CaM at 22 °C also produced virtually no change in the extent of dantrolene inhibition of DP4-induced domain unzipping.

Inhibition of Skeletal Muscle SR Ryanodine Binding and Ca^{2+} Release by Dantrolene—Ryanodine binds to RyRs only when the channel is in the open state, and the degree of ryanodine binding is widely used as a biochemical measure of the degree of channel activation (44). Fig. 5 shows the concentration-dependent effects of DP4 or DP4-mut on [^{3}H]ryanodine binding at 22 °C. In these experiments, MCA-labeled SR was used to correlate the physiological properties of the Ca^{2+} channel with the fluorescence quenching data. MCA-labeled and -unlabeled SR preparations showed essentially the same responses to DP4, dantrolene, and the other effectors (data not shown). Fig. 5 demonstrates that DP4 enhanced [^{3}H]ryanodine binding to the SR in a concentration-dependent manner. Comparison of Figs. 3*C* and 5 reveals that the enhancement of [^{3}H]ryanodine binding and fluorescence quenching occurred in approximately the same concentration range of DP4. This indicates that unzipping of the domain switch and activation of Ca^{2+} channels are well coordinated. Surprisingly, 10 μM dantrolene caused little inhibition of [^{3}H]ryanodine binding at 22 °C (Table II). At this temperature, dantrolene inhibition, if any, was not more than 10% of the control at all concentrations of DP4 tested (data not shown). CaM alone (1 μM) increased the specific activity of [^{3}H]ryanodine binding to the SR at 22 °C, but dantrolene was now able to significantly suppress radioligand binding (~35%) (Table II). When we carried out the same type of experiments at 37 °C, dantrolene produced equivalently significant inhibition of [^{3}H]ryanodine binding (~59%) in the presence or absence of CaM, in agreement with previous reports (7, 12, 13, 45). These results suggest that higher temperature and CaM have similar effects on the extent of dantrolene inhibition of DP4-induced activation of RyR Ca^{2+} channels. These effects of temperature and CaM on the extent of

TABLE I

Dantrolene inhibition of DP4-induced macromolecular fluorescence quenching of MCA-labeled RyR1: effects of temperature and CaM

The K_Q'/K_Q values were determined in the absence or presence of 10 μM dantrolene at 22 and 37 °C to examine the effect of dantrolene on domain unzipping (K_Q'/K_Q) induced by 100 μM DP4. The same experiments were carried out in the presence of 1 μM CaM. Each datum point represents the mean ± S.D. The number of experiments is shown in parentheses. A paired *t* test was employed to determine the statistical significance of the data (*p* value). ND, not determined.

	K_Q'/K_Q	
	22 °C	37 °C
100 μM DP4	1.76 ± 0.09 (7)	1.82 ± 0.03 (5)
100 μM DP4 + 10 μM dantrolene	1.20 ± 0.07 (7)[a]	1.16 ± 0.06 (5)[a]
Inhibition (%)	73.7 ± 10.9 (7)	80.9 ± 7.4 (5)
100 μM DP4 + 1 μM CaM	1.80 ± 0.09 (6)	ND
100 μM DP4 + 1 μM CaM + 10 μM dantrolene	1.21 ± 0.07 (6)[b]	ND
Inhibition (%)	74.3 ± 8.7 (6)	ND

[a] $p < 0.05$ *versus* 100 μM DP4.
[b] $p < 0.05$ *versus* 100 μM DP4 + 1 μM CaM.

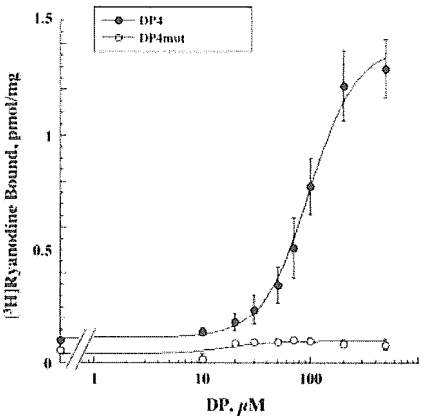

FIG. 5. **DP4-induced activation of [³H]ryanodine binding *versus* DP4 or DP4-mut concentration at 22 °C.** The data were fitted to the equation $y = aK^2x^2/(1 + K^2x^2)$, where y is the amount of ryanodine bound at x concentration of DP4, a is the maximal binding, and K is the association constant. Each datum point represents the mean ± S.D. of at least four experiments carried out in duplicate.

dantrolene inhibition of RyR Ca^{2+} channels are in sharp contrast to the lack of effect of these factors on the extent of dantrolene inhibition of fluorescence quenching.

Our data above (Fig. 2*B*) demonstrate that DP4-mut had virtually no effect on fluorescence quenching. This suggests that MH mutations in DP4 destroy the ability of this sequence to bind to its mating domain on the N-terminal region of RyR1. Accordingly, there should be no channel activation by DP4-mut, as was indeed demonstrated by the inability of this mutated peptide to enhance [³H]ryanodine binding at 22 °C (Fig. 5) and at 37 °C (data not shown). Taken together, our results suggest (*a*) that domain unzipping is a prerequisite for DP4-induced channel opening, (*b*) that dantrolene exerts its inhibitory action directly upon the domain switch, and (*c*) that the inhibition signal elicited in the domain switch is transmitted to the Ca^{2+} channel in a temperature- and CaM-dependent manner.

We next investigated the effect of temperature and CaM on the ability of dantrolene to inhibit DP4-induced SR Ca^{2+} release, as measured by the time- and Ca^{2+}-dependent changes in fluo-3 fluorescence spectrophotometry (Fig. 6). These Ca^{2+} release experiments were carried out with an MCA-unlabeled SR preparation because MCA labeling did not produce appreciable changes in the RyR properties in preliminary experiments (data not shown). Approximately 20 s after Ca^{2+} uptake was initiated by the addition of MgATP, 100 μM DP4 was added to induce Ca^{2+} release, and the effect of 10 μM dantrolene on the Ca^{2+} release time course in the absence and presence of 1 μM CaM was analyzed. The Ca^{2+} release time courses (shown in Fig. 6) were fitted to a double exponential equation: $y = y_0 + a(1 - e^{-k_1t}) + b(1 - e^{-k_2t})$, where a and b are the magnitude of the fast and slow phases of release, respectively; and k_1 and k_2 are the rate constants of the fast and slow phases, respectively. The calculated values of the initial rate of Ca^{2+} release ($(dy/dt)_{t>0} = ak_1 + bk_2$) and the amount of Ca^{2+} release ($a + b$) are listed in Table III. At 22 °C and in the absence of CaM, dantrolene produced no appreciable effect on the initial rate of Ca^{2+} release, although there was a small but appreciable inhibition of the slow phase of Ca^{2+} release (Fig. 6*A* and Table III). The addition of 1 μM CaM resulted in a significant increase in the initial rate of Ca^{2+} release. Under these conditions, 10 μM dantrolene produced a significant reduction in the initial rate (~ 41%) and an appreciable reduction in the total amount of Ca^{2+} released, as well. Interestingly, raising the experimental temperature to 37 °C produced an effect similar in magnitude to that produced by CaM at 22 °C. Thus, at 37 °C, dantrolene produced a significant reduction in both the initial rate and the amount of Ca^{2+} release even in the absence of CaM. These results are again consistent with the view that CaM and temperature seem to affect the dantrolene-blocking signal from the domain switch to the Ca^{2+} channel pore domain.

DISCUSSION

Dantrolene acts as an intracellular skeletal muscle relaxant and is the primary therapeutic agent used for the treatment of MH (46). A considerable amount of information accumulated in the literature suggests that, at micromolar concentrations, dantrolene blocks some step(s) of activation of RyR1 Ca^{2+} channels, but the detailed mechanism of its pharmacological action remains obscure. The main aim of this study was to gain a deeper insight into the molecular mechanism of the pharmacological action of dantrolene.

We proposed the domain switch model to explain both the mechanism of channel activation under normal conditions and the mechanism of pathogenesis of channel dysfunction. The model assumes that the mode of interaction between the N-terminal and central domains of the RyR (the two major regions harboring many of the reported MH mutations) is involved in Ca^{2+} channel regulation and also in the pathogenesis of MH. In the resting state, the two domains make close contact at several subdomains forming the zipped configuration (*i.e.* the "off" configuration of the on/off switch), and this configuration stabilizes the closed state of the Ca^{2+} channel. Stimulation of the RyR by T tubule depolarization or chemical agonists causes unzipping of the domain switch (the "on" configuration of the switch), leading to Ca^{2+} channel opening. Mutations in conformationally active portions of either region of the domain switch weaken the interdomain interactions, causing partial unzipping of the switch. As a result, MH-susceptible RyR1 channels are more readily opened as manifested in hyperactivation/hypersensitization effects. In our recent studies, the domain switch hypothesis was tested by examining the effects of synthetic peptides corresponding to the

TABLE II

Dantrolene inhibition of DP4-induced enhancement of [^{3}H]ryanodine binding activity: effects of temperature and CaM

[^{3}H]Ryanodine binding to skeletal muscle SR vesicles was determined in the absence or presence of 10 μM dantrolene at 22 or 37 °C as described under "Experimental Procedures." The same experiments were carried out in the presence of 1 μM CaM. Each datum point represents the mean ± S.D. The number of experiments is shown in parentheses. A paired *t* test was employed to determine the statistical significance of the data (*p* value).

	[^{3}H]Ryanodine bound	
	22 °C	37 °C
	pmol/mg	
100 μM DP4	0.76 ± 0.07 (12)	0.64 ± 0.18 (6)
100 μM DP4 + 10 μM dantrolene	0.72 ± 0.04 (10)	0.26 ± 0.06 (6)[a]
Inhibition (%)	5.5 ± 18.1 (10)	59.1 ± 9.3 (6)
100 μM DP4 + 1 μM CaM	1.95 ± 0.46 (6)[a]	1.85 ± 0.26 (6)[a]
100 μM DP4 + 1 μM CaM + 10 μM dantrolene	1.28 ± 0.16 (6)[b]	0.75 ± 0.11 (6)[b]
Inhibition (%)	34.5 ± 13.2 (6)	59.2 ± 6.2 (6)

[a] $p < 0.05$ *versus* 100 μM DP4.
[b] $p < 0.05$ *versus* 100 μM DP4 + 1 μM CaM.

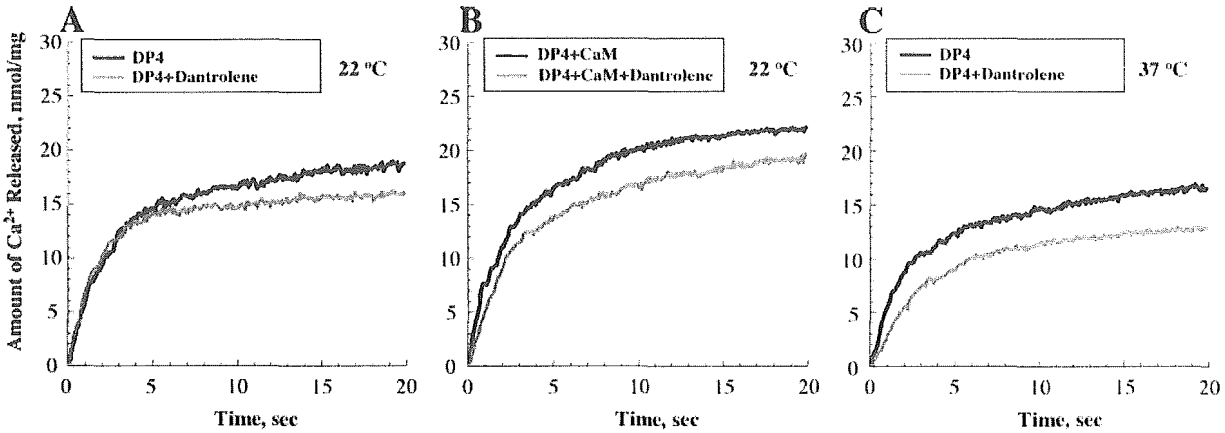

FIG. 6. **Dantrolene inhibits DP4-induced Ca^{2+} release with a temperature and CaM dependence.** *A*, time course of DP4-induced Ca^{2+} release in the absence of dantrolene (*black trace*) and in the presence of 10 μM dantrolene (*gray trace*) at 22 °C. After the Ca^{2+} uptake initiated by the addition of 1 mM MgATP had reached a plateau, various concentrations of DP4 were added, and the resultant Ca^{2+} release was monitored by fluo-3 fluorescence spectrophotometry. *B*, the same experiment as described for *A*, except that 1 μM CaM was present during the course of the Ca^{2+} release experiment. *C*, the same experiment as described for A, except that it was carried out at 37 °C. Each Ca^{2+} release trace presented here was obtained by signal averaging a total of 35–75 traces originating from four to seven experiments.

TABLE III

Inhibition of SR Ca^{2+} release by dantrolene: effects of temperature and CaM

The initial rate ($ak_1 + bk_2$) of Ca^{2+} release was calculated by fitting a double exponential function ($y = y_0 + a(1 - e^{-k_1 t}) + b(1 - e^{-k_2 t})$, where *a* and *b* are the magnitude of the fast and slow phases of release, respectively; and k_1 and k_2 are the rate constants of the fast and slow phases, respectively) to the first 20 s of the time course of fluo-3 fluorescence change after the addition of DP4. Each datum point represents the mean ± S.D. The number of experiments is shown in parentheses. A paired *t* test was employed to determine the statistical significance of the data (*p* value). ND, not determined.

	Initial rate ($ak_1 + bk_2$)		Total Ca^{2+} release ($a + b$)	
	22 °C	37 °C	22 °C	37 °C
	nmol/mg/s			
100 μM DP4	7.86 ± 1.75 (5)	6.79 ± 0.47 (5)	19.49 ± 2.66 (5)	18.34 ± 0.95 (5)
100 μM DP4 +10 μM dantrolene	8.53 ± 1.03 (4)	3.35 ± 0.97 (6)[a]	17.38 ± 1.18 (4)	16.08 ± 1.11 (6)[a]
Inhibition (%)	−8.5 ± 12.9 (4)	50.7 ± 14.3 (6)	10.8 ± 12.9 (4)	12.3 ± 6.1 (6)
100 μM DP4 + 1 μM CaM	12.02 ± 3.11 (7)[a]	ND	22.43 ± 0.83 (7)[a]	ND
100 μM DP4 + 1 μM CaM + 10 μM dantrolene	7.07 ± 1.11 (6)[b]	ND	20.60 ± 0.65 (6)[b]	ND
Inhibition (%)	41.2 ± 8.8 (6)	ND	8.0 ± 2.9 (6)	ND

[a] $p < 0.05$ *versus* 100 μM DP4.
[b] $p < 0.05$ *versus* 100 μM DP4 + 1 μM CaM.

putative critical domains of the RyR (domain peptides) and antibodies raised against these domain peptides. DP4 enhances ryanodine binding (28), induces Ca^{2+} release from the SR (29), induces contraction in skinned muscle fibers at an inhibitory Mg^{2+} concentration (41), increases the sensitivity to caffeine (41), increases the frequency of Ca^{2+} sparks in saponin-permeabilized fibers (42), and increases the open probability of single channels (42). Similarly, anti-DP4 polyclonal antibody, directed against the Leu^{2442}–Pro^{2477} region (a portion of the central domain) of RyR1, produces hyperactivation of Ca^{2+} channels and hypersensitization of Ca^{2+} channels to agonists (31).

The most important aspect of this study is the finding that dantrolene inhibits the DP4-induced increase in K_Q, *i.e.* dantrolene stabilizes a zipped configuration of the domain switch even in the presence of domain-unzipping agents such as DP4 and anti-DP4 antibody. Since domain unzipping produced by DP4 or anti-DP4 antibody seems to simulate the channel dysfunction caused by MH mutations, the present findings suggest that the molecular mechanism of therapeutic action of dantrolene in MH is to stabilize a zipped configuration of the

domain switch, despite the tendency of the mutation to destabilize the domain switch. As a result, the channel hyperactivity and hypersensitivity caused by MH mutations are suppressed by dantrolene. Since the dantrolene-binding site is located in the Leu^{590}–Cys^{609} region of the proposed RyR1 domain switch (37), interdomain stabilization by dantrolene must be produced by direct binding of the drug to a region of the domain switch.

In agreement with previous reports (7, 12, 13, 45, 46), we found that the extent of dantrolene inhibition of DP4-induced RyR1 channel activation, as determined by both [^{3}H]ryanodine binding and SR Ca^{2+} release, varies with the temperature, *i.e.* significant inhibition was observed at 37 °C, with only negligible inhibition at 22 °C. An interesting new finding in this study is that dantrolene inhibition of DP4-induced domain unzipping is independent of temperature. Thus, it seems that the requirement for physiological temperatures for dantrolene activity is not due to a temperature dependence for the stabilization of a zipped configuration of the domain switch. Rather, the temperature requirement is for the downstream mechanism(s) of actual channel opening. According to our working hypothesis, the on/off signal elicited in the domain switch is transmitted to the putative channel gating/pore domain by mediation of some intraprotein coupling mechanism that requires higher temperatures for activation or inhibition.

According to an earlier report (13), the addition of CaM is required to observe dantrolene inhibition of RyR1 channel function. We addressed the question of the possible role of CaM in modulating dantrolene activity in this study. We detected no further effect of CaM on dantrolene inhibition of ryanodine binding or Ca^{2+} release at 37 °C, where there was already significant inhibition by dantrolene. However, at 22 °C, where there was very little dantrolene intrinsic inhibition, the extent of dantrolene inhibition of both ryanodine binding and Ca^{2+} release was considerably increased in the presence of CaM. At 22 °C, however, CaM had no effect on the extent of dantrolene inhibition of domain unzipping. These results suggest that, like raising the temperature from 22 to 37 °C, CaM may lower the conformational energy barrier for the proposed coupling between the domain switch and the channel gating/pore domain and enhance blocking signals elicited in the domain switch to more effectively transmit them to the functional Ca^{2+} channel. These results further suggest that the CaM-binding site on RyR1 is an intervening domain that mediates inhibitory signals from the domain switch to the channel gating/pore domain. Clearly, more work is required to elucidate the detailed molecular mechanism of pharmacological and therapeutic actions of dantrolene.

In summary, we speculate that dantrolene binding to the Leu^{590}–Cys^{609} region of the N-terminal portion of the domain switch produces a local conformational change that results in reinforcement of the interdomain interactions between itself and its mating subdomain, likely located within the central domain portion of the domain switch. This stabilizes a zipped (*i.e.* closed) configuration. Thus, further characterization of the domain-domain interactions involving the dantrolene-binding region will be significant for further resolution of the molecular mechanism of dantrolene action on RyR1 in health and disease, as well as the mechanism of intraprotein control of channel opening.

Acknowledgments—We thank Dr. Renne C. Lu, Dr. Paul Leavis, David Schrier, and Elizabeth Gowell for help in the synthesis and purification of the peptides.

REFERENCES

1. Mickelson, J. R., and Louis, C. F. (1996) *Physiol. Rev.* **76,** 537–592
2. Ellis, K. O., Castellion, A. W., Honkomp, L. J., Wessels, F. L., Carpenter, J. E., and Halliday, R. P. (1973) *J. Pharmacol. Sci.* **62,** 948–995
3. Szentesi, P., Collet, C., Sarkozi, S., Szegedi, C., Jona, I., Jacquemond, V., Kovacs, L., and Csernoch, L. (2001) *J. Gen. Physiol.* **118,** 355–375
4. Gallant, E. M., and Lentz, L. R. (1992) *Neurosci. Lett.* **28,** 181–186
5. Flewellen, E. H., Nelson, T. E., Jones, W. P., Arens, J. F., and Wagner, D. I. (1983) *Anesthesiology* **59,** 275–280
6. Hainaut, K., and Desmedt, J. E. (1974) *Nature* **252,** 728–730
7. Morgan, K. G., and Bryant, S. H. (1977) *J. Pharmacol. Exp. Ther.* **201,** 138–147
8. Owen, B. J., Taske, N. L., and Lamb, G. D. (1997) *Am. J. Physiol.* **272,** C203–C211
9. Lamb, G. D. (1993) *J. Muscle Res. Cell Motil.* **14,** 554–556
10. Van Winkle, W. B. (1976) *Science* **193,** 1130–1131
11. Herbette, L., Messineo, F. C., and Katz, A. M. (1982) *Annu. Rev. Pharmacol.* **22,** 413–434
12. Otha, T., Ito, S., and Ohga, A. (1990) *Eur. J. Pharmacol.* **178,** 11–19
13. Fruen, B. R., Mickelson, J. R., and Louis, C. F. (1997) *J. Biol. Chem.* **272,** 26965–26971
14. Zhao, F., Li, P., Chen, S. R., Louis, C. F., and Fruen, B. R. (2001) *J. Biol. Chem.* **276,** 13810–13816
15. Palnitkar, S. S., Mickelson, J. R., Louis, C. F., and Parness, J. (1997) *Biochem. J.* **326,** 847–852
16. Nelson, T. E., Lin, M., Zaoata-Sudo, G., and Sudo, R. T. (1996) *Anesthesiology* **84,** 1368–1379
17. Britt, B. A., Scott, E., Frodis, W., Clements, M. J., and Endrenyi, L. (1984) *Can. Anaesth. Soc. J.* **31,** 130–154
18. Ohnishi, S. T., Taylor, S., and Gronert, G. A. (1983) *FEBS Lett.* **161,** 103–107
19. Dirksen, R. T., and Avila, G. (2002) *Trends Cardiovasc. Med.* **12,** 189–197
20. Galli, L., Orrico, A., Cozzolino, S., Pietrini, V., Tegazzin, V., and Sorrentino, V. (2002) *Cell Calcium* **32,** 143–151
21. Davis, M. R., Haan, E., Jungbluth, H., Sewry, C., North, K., Muntoni, F., Kuntzer, T., Lamont, P., Bankier, A., Tomlinson, P., Sanchez, A., Walsh, P., Nagarajan, L., Oley, C., Colley, A., Gedeon, A., Quinlivan, R., Dixon, J., James, D., Muller, C. R., and Laing, N. G. (2003) *Neuromuscul. Disord.* **13,** 151–157
22. Monnier, N., Ferreiro, A., Marty, I., Labarre-Vila, A., Mezin, P., and Lunardi, J. (2003) *Hum. Mol. Genet.* **12,** 1171–1178
23. Zorzato, F., Yamaguchi, N., Xu, L., Meissner, G., Muller, C. R., Pouliquin, P., Muntoni, F., Sewry, C., Girard, T., and Treves, S. (2003) *Hum. Mol. Genet.* **12,** 379–388
24. Tammaro, A., Bracco, A., Cozzolino, S., Esposito, M., Di Martino, A., Savoia, G., Zeuli, L., Piluso, G., Aurino, S., and Nigro, V. (2003) *Clin. Chem.* **49,** 761–768
25. Avila, G., O'Connell, K. M., and Dirksen, R. T. (2003) *J. Gen. Physiol.* **121,** 277–286
26. Du, G. G., Khanna, V. K., Guo, X., and MacLennan, D. H. (2004) *Biochem. J.* **382,** 557–564
27. Yang, T., Ta, T. A., Pessah, I. N., and Allen, P. D. (2003) *J. Biol. Chem.* **278,** 25722–25730
28. Yamamoto, T., El-Hayek, R., and Ikemoto, N. (2000) *J. Biol. Chem.* **275,** 11618–11625
29. Yamamoto, T., and Ikemoto, N. (2002) *Biochemistry* **41,** 1492–1501
30. Ikemoto, N., and Yamamoto, T. (2002) *Front. Biosci.* **7,** 671–683
31. Kobayashi, S., Yamamoto, T., Parness, J., and Ikemoto N. (2004) *Biochem. J.* **380,** 561–569
32. Palnitkar, S. S., Bin, B., Jimenez, L. S., Morimoto, H., Williams, P. G., Paul-Pletzer, K., and Parness, J. (1999) *J. Med. Chem.* **42,** 1872–1880
33. Paul-Pletzer, K., Palnitkar, S. S., Jiminez, L. S., Morimoto, H., and Parness, J. (2001) *Biochemistry* **40,** 531–542
34. Paul-Pletzer, K., Yamamoto, T., Bhat, M. B., Ma, J., Ikemoto, N., Jimenez, L. S., Morimoto, H., Williams, P. G., and Parness, J. (2002) *J. Biol. Chem.* **277,** 34918–34923
35. Ikemoto, N., Kim, D. H., and Antoniu, B. (1988) *Methods Enzymol.* **157,** 469–480
36. Kang, J. J., Tarcsafalvi, A., Carlos, A. D., Fujimoto, E., Shahrokh, Z., Thevenin, B. J., Shohet, S. B., and Ikemoto, N. (1992) *Biochemistry* **31,** 3288–3293
37. Inui, M., and Fleischer, S. (1988) *Methods Enzymol.* **157,** 490–505
38. El-Hayek, R., Lokuta, A. J., Arevalo, C., and Valdivia, H. H. (1995) *J. Biol. Chem.* **270,** 28696–28704
39. Chen, S. R., Airey, J. A., and MacLennan, D. H. (1993) *J. Biol. Chem.* **268,** 22642–22649
40. Wu, Y., Aghdasi, B., Dou, S. J., Zhang, J. Z., Liu, S. Q., and Hamilton, S. L. (1997) *J. Biol. Chem.* **272,** 25051–25061
41. Lamb, G. D., Posterino, G. S., Yamamoto, T., and Ikemoto, N. (2001) *Am. J. Physiol.* **281,** C207–C214
42. Shtifman, A., Ward, C. W., Yamamoto, T., Wang, J., Olbinski, B., Valdivia, H. H., Ikemoto, N., and Schneider, M. F. (2002) *J. Gen. Physiol.* **116,** 15–31
43. Parness, J., and Palnitkar, S. S. (1995) *J. Biol. Chem.* **270,** 18465–18472
44. Meissner, G. (1994) *Annu. Rev. Physiol.* **56,** 458–508
45. Ohta, T., Endo, M., Morohoshi, Y., Wanikawa, K., and Ohga, A. (1989) *Am. J. Physiol.* **256,** C358–C367
46. Krause, T., Gerbershagen, M. U., Fiege, M., Weisshorn, R., and Wappler, F. (2004) *Anaesthesia* **59,** 364–373

Safety and Efficacy of Repeated Sauna Bathing in Patients With Chronic Systolic Heart Failure: A Preliminary Report

HIROMITSU MIYAMOTO, MD,[1] HISASHI KAI, MD, PhD,[1,2] HIROYUKI NAKAURA, MD, PhD,[1] KATSUNORI OSADA, MD,[1] YOSHIHIKO MIZUTA, MD,[1] AKIRA MATSUMOTO, MD, PhD,[1] AND TSUTOMU IMAIZUMI, MD, PhD[1,2]

Kurume, Japan

ABSTRACT

Background: We sought to determine the safety and efficacy of repeated 60°C sauna bathing in patients with chronic systolic congestive heart failure (CHF).

Methods and Results: This study included 15 hospitalized CHF patients (New York Heart Association class = 2.8 ± 0.4) in stable clinical condition on conventional treatments. Sauna bathing was performed once per day for 4 weeks. Repeated sauna bathing was safely completed without any adverse effects in all patients. Symptoms improved in 13 of 15 patients after 4 weeks. Sauna bathing decreased systolic blood pressure without affecting heart rate, resulting in significant decrease in the rate-pressure product (6811 ± 1323 to 6292 ± 1093). Echocardiographic left ventricular ejection fraction was significantly increased from 30 ± 11 to 34 ± 11%. Sauna bathing significantly improved exercise tolerance manifested by prolonged 6-minute walking distance (388 ± 110 to 448 ± 118 m), increased peak respiratory oxygen uptake (13.3 ± 1.8 to 16.3 ± 2.1 mL/kg/min), and enhanced anaerobic threshold (9.4 ± 1.2 to 11.5 ± 1.9 mL/kg/min). Four-week bathing significantly reduced plasma epinephrine (40 ± 42 to 21 ± 23 pg/mL) and norepinephrine (633 ± 285 to 443 ± 292 pg/mL). Sauna bathing reduced the number of hospital admission for CHF (2.5 ± 1.3 to 0.6 ± 0.8 per year).

Conclusion: Repeated 60°C sauna bathing was safe and improved symptoms and exercise tolerance in chronic CHF patients. Sauna bathing may be an effective adjunctive therapy for chronic systolic CHF.

Key Words: Thermal therapy, exercise tolerance, echocardiography, catecholamines.

The primary therapeutic goals of chronic congestive heart failure (CHF) are improvement of prognosis and maintenance of quality of life. In this regard, great progress has been achieved by recent advances in pharmacologic treatment using angiotensin-converting enzyme inhibitors,[1,2] angiotensin II receptor blockers,[3,4] β-blockers,[5,6] and aldosterone antagonists.[7] However, many patients on conventional treatment still have impaired quality of life. Therefore, some other modalities of treatment are desirable.

Cardiovascular responses to ordinary hot (80°C) sauna include tachycardia, systolic hypertension, and increased cardiac workload, which are mediated by peripheral vasodilatation and stimulation of the sympathetic nerve system.[8–10] These changes are similar to the response to heat stress. Thus hot sauna bathing is considered to be inappropriate or harmful for CHF patients. However, Tei et al[11] have demonstrated that a single 60°C dry sauna bathing for 15 minutes was tolerable to CHF patients and produced beneficial acute hemodynamic effects, such as increase in cardiac output and decreases in systemic vascular resistance and pulmonary capillary wedge pressure via thermal peripheral vasodilatation. In addition, the same group showed that repeated 60°C sauna bathing for 2 weeks improved subjective well-being and the forearm endothelial function in CHF patients.[12] However, there were no reports on the effects of repeated sauna bathing on the exercise tolerance. Accordingly, the safety and efficacy of repeated 60°C sauna bathing for 4 weeks were investigated in patients with systolic chronic CHF on conventional treatment. For these purposes, we determined the effects of sauna bathing on clinical symptoms, exercise tolerance, neurohumoral factors, and echocardiographic left ventricular ejection fraction (LVEF).

From [1]The Third Department of Internal Medicine and [2]Cardiovascular Research Institute, Kurume University School of Medicine, Kurume, Japan

Manuscript received October 21, 2004; revised manuscript received March 10, 2005; revised manuscript accepted March 11, 2005.

Reprint requests: Hisashi Kai, MD, PhD, The Third Department of Internal Medicine and Cardiovascular Research Institute, Kurume University School of Medicine, 67 Asahimachi, Kurume 830-0011, Japan.

Partially supported and by a Grant-in-Aid for Scientific Research and by a grant for Academic Frontier Project from the Ministry of Education, Science, Sports, Culture, and Technology, Japan.

1071-9164/$ - see front matter

doi:10.1016/j.cardfail.2005.03.004